TECHNICAL REPORT
NATICK/TR-18/014

AD _____

AMPHIPHILIC BLOCK COPOLYMER THIN FILM THAT SIMULTANEOUSLY BALANCES MULTIPLE ORTHOGONAL FUNCTIONS

by
Timothy J. Lawton
Joshua R. Uzarski
and
Shaun F. Filocamo

September 2018

Final Report
May 2014 – May 2016

U.S. Army Natick Soldier Research, Development and Engineering Center
Natick, Massachusetts 01760-5000

DISCLAIMERS

The findings contained in this report are not to be construed as an official Department of the Army position unless so designated by other authorized documents.

Citation of trade names in this report does not constitute an official endorsement or approval of the use of such items.

DESTRUCTION NOTICE

For Classified Documents:

Follow the procedures in DoD 5200.22-M, Industrial Security Manual, Section II-19 or DoD 5200.1-R, Information Security Program Regulation, Chapter IX.

For Unclassified/Limited Distribution Documents:

Destroy by any method that prevents disclosure of contents or reconstruction of the document.

REPORT DOCUMENTATION PAGE

Form Approved
OMB No. 0704-0188

PLEASE DO NOT RETURN YOUR FORM TO THE ABOVE ADDRESS.

1. REPORT DATE *(DD-MM-YYYY)*	2. REPORT TYPE	3. DATES COVERED *(From - To)*
06-09-2018	Final	May 2014 – May 2016

4. TITLE AND SUBTITLE

AMPHIPHILIC BLOCK COPOLYMER THIN FILM THAT SIMULTANEOUSLY BALANCES MULTIPLE ORTHOGONAL FUNCTIONS

5a. CONTRACT NUMBER

5b. GRANT NUMBER

5c. PROGRAM ELEMENT NUMBER

6. AUTHOR(S)

Timothy J. Lawton,* Joshua R. Uzarski, and Shaun F. Filocamo

5d. PROJECT NUMBER

5e. TASK NUMBER

5f. WORK UNIT NUMBER

7. PERFORMING ORGANIZATION NAME(S) AND ADDRESS(ES)

U.S. Army Natick Soldier Research, Development and Engineering Center
ATTN: RDNS-SEW-TMS
15 General Greene Avenue, Natick, MA 01760-5000

8. PERFORMING ORGANIZATION REPORT NUMBER

NATICK/TR-18/014

9. SPONSORING / MONITORING AGENCY NAME(S) AND ADDRESS(ES)

10. SPONSOR/MONITOR'S ACRONYM(S)

11. SPONSOR/MONITOR'S REPORT NUMBER(S)

12. DISTRIBUTION / AVAILABILITY STATEMENT

Approved for public release; distribution is unlimited.

13. SUPPLEMENTARY NOTES

* This research was performed while the author (TJL) held a CBD-NRC Research Associateship award at U.S. Army Natick Soldier Research, Development & Engineering Center. The authors greatly appreciate the funding from U.S. Army Natick Soldier Research, Development & Engineering Center.

14. ABSTRACT

When creating a multifunctional surface, issues can arise when having functions exist simultaneously, especially when the functions are incongruent. In this report, a range of surface compositions are determined that simultaneously support the orthogonal functions of water repellency and enzyme activity. The multifunctional surface is made by spin-coating a solution of an amphiphilic block copolymer (polystyrene-block-poly(acrylic acid)) into a thin film. In solution, the block copolymer self-assembles into micelles, so that after spin-coating the copolymer film contains microphase-separated hydrophilic and hydrophobic domains. The hydrophobic domains support water repellency and the hydrophilic cores of the micelles are used to immobilize enzymes. To characterize the composition, wettability and activity of the surfaces, atomic force microscopy (AFM), contact angle goniometry and enzyme assays are used. From these techniques, the density was determined of hydrophilic sites amongst the hydrophobic background of the amphiphilic surface that maximized both functions simultaneously.

15. SUBJECT TERMS

GOLD	ASSAYING	WETTABILITY	ENZYME ACTIVITY
ASSAYS	CASTINGS	SELF ASSEMBLY	MULTIFUNCTIONAL
ENZYMES	THIN FILMS	FLUORESCENCE	SOLUTION CASTING
MICELLES	SPIN COATED	ENZYME ASSAYS	WATER REPELLENTS
SURFACES	SPIN COATING	CONTACT ANGLE	BLOCK COPOLYMERS
MULTIFUNCTIONALITY		ORTHOGONAL FUNCTIONS	

16. SECURITY CLASSIFICATION OF:			17. LIMITATION OF ABSTRACT	18. NUMBER OF PAGES	19a. NAME OF RESPONSIBLE PERSON
a. REPORT	b. ABSTRACT	c. THIS PAGE			Timothy Lawton
U	U	U	UU	24	19b. TELEPHONE NUMBER *(include area code)* (508) 233-4193

Standard Form 298 (Rev. 8-98)
Prescribed by ANSI Std. Z39.18

This page intentionally left blank

Table of Contents

List of Figures iv
Preface v
Acknowledgements vi
1. Introduction 1
2. Materials and Methods 3
2.1 Materials 3
2.2 Instrumentation 3
2.3 Methods 3
2.3.1 Creating Mixed PS-b-PAA & PS Solutions 3
2.3.2 Surface Cleaning Procedure 4
2.3.3 Layer-by-Layer and Spin-Coating Procedure 4
2.3.4 Enzyme Immobilization and Assay 5
3. Results and Discussion 6
3.1 Determining Micelle Density 6
3.2 Measuring the Water Repellency Function 8
3.3 Measuring the Enzyme Activity Function 10
3.4 Determining Surface Composition Needed for Simultaneous Multifunctionality 12
4. Conclusion 14
5. References 15

List of Figures

Figure 1. Schematic for the preparation of PS:PS-b-PAA polymer thin films with immobilized HRP. 4
Figure 2. AFM topography images of a PS-b-PAA block copolymer film after spin coating (A) reveal spherical micelles. After soaking in NaOH solution (B) the spherical micelles have a depression in the middle, forming cavities. Images are 1 x 1 μm^2. Inset in (A) is zoomed in region showing the pseudo-hexagonal packing of the as-cast micelles. Inset is 0.1 x 0.1 μm^2 6
Figure 3. AFM topography images of surfaces cast from solutions containing different mole ratios of pure PS to the PS-b-PAA block copolymer. (A) 2:1 (B) 5:1 (C) 10:1 and (D) 25:1. All images are 1 x 1 μm^2 8
Figure 4. Micelle density as a function of PS:PS-b-PAA. The micelle density was determined by counting the number of micelles per area over 6 μm^2 for each solution on multiple chips. Error bars are the standard deviation of density measurements. 8
Figure 5. Left Y axis, contact angle measurements for different PS:PS-b-PAA ratios after spin coating and soaking in NaOH. Right Y axis, roughness measurements collected via AFM. The arrows in the graph point to the appropriate axis for each set of data points. Error bars are the standard deviation of the measurements for each data point 9
Figure 6. Contact angle measurements pre- (white) and post- (gray) exposure to HRP and washing. In the Post-HRP data set, the contact angle is plateauing between the 2:1 and 5:1 surfaces. Error bars are the standard deviation of the measurements for each data point 10
Figure 7. HRP fluorescence assay for the different PS:PS-b-PAA surfaces. Fluorescence, measured in RFU, was collected at specified time points for all surfaces. Error bars are the standard deviation of the mean. 11
Figure 8. Comparison of the total product formed during 60 min reaction time, in moles (Left Y axis) and the contact angle after HRP immobilization and washing (Right Y axis). Error bars are the standard deviation of the measurements for each data point 12

Preface

This technical report documents the progress made on research conducted during a two-year period of a National Research Council (NRC) Fellowship sponsored by the Defense Threat Reduction Agency (DTRA) in their Chemical/Biological Defense (CBD) mission area. The research focused on creating multifunctional thin films from spin coating solutions of amphiphilic block copolymers. Throughout the two year period from May 2014 – May 2016, thin films were created and analyzed to determine whether they exhibited simultaneous multifunctionality of enzyme activity and water repellency. The films were cast onto gold-coated surfaces and were characterized with a number of surface-sensitive techniques. This research and development project was conducted at the U.S. Army Natick Soldier Research, Development and Engineering Center (NSRDEC).

Acknowledgements

This research was performed while Timothy J. Lawton held a CBD-NRC Research Associateship award at U.S. Army Natick Soldier Research, Development and Engineering Center. The authors greatly appreciate the support from U.S. Army Natick Soldier Research, Development and Engineering Center.

AMPHIPHILIC BLOCK COPOLYMER THIN FILM THAT SIMULTANEOUSLY BALANCES MULTIPLE ORTHOGONAL FUNCTIONS

1. Introduction

This report presents results and findings from research conducted at the U.S. Army Natick Soldier Research, Development and Engineering Center (NSRDEC) to create a multifunctional surface from an amphiphilic block copolymer thin film. The work was performed from May 2014 – May 2016 by a postdoctoral research fellow sponsored by the Defense Threat Reduction Agency's Chemical/Biological Defense (DTRA-CBD) mission area.

In the field of multifunctional interfaces, diblock copolymers offer a novel route to creating a surface coating exhibiting several simultaneously active functions. Diblock copolymers are blocks of repeating units of two different, often immiscible, polymers covalently bound together [1]. Since the blocks are covalently bound together, they cannot macroscopically separate into large discrete domains when dissolved in solvent, as they would when isolated. Instead, they will aggregate via self-assembly and microphase separate leading to the formation of a variety of shapes and sizes depending on the length and ratio of the blocks and the nature of the solvent [2]. These copolymer shapes can include micelles, vesicles, lamellae and plates [3]. Block copolymer aggregates, especially vesicles and micelles, have been explored for a number of applications including drug delivery and enzyme activity [4-5]. By casting these aggregates into films it is possible to create spatially separated domains with different chemical reactivity that can support multifunctionality [6].

Block copolymer surfaces have shown promise as multifunctional interfaces in fields ranging from nanoparticle synthesis [7-8] to nanobioarrays [9] to supports for enzyme immobilization [10]. Unlike other multifunctional interfaces created from alkanethiol self-assembled monolayers (SAMs) and lithography techniques, block copolymer thin films can be formed on a variety of non-noble metal surfaces and without costly and time-consuming fabrication equipment [11]. While there is precedent for using block copolymers to control surface wettability [12] and enzyme immobilization to a single block within that film [13-15], it is still unclear if these surfaces can simultaneously balance orthogonal functions such as hydrophilic enzyme activity and water repellency.

Studies of enzyme immobilization onto copolymer surfaces have shown that it is a method capable of improving enzyme recoverability and selectivity while maintaining up to 85% of the free enzyme activity [15-16]. Additionally, by immobilizing enzymes to copolymer surfaces it is possible to stabilize them for longer in more extreme temperature and pH conditions than the free enzyme [10]. The improved stability is especially desirable because many enzyme applications require them to be in an unnatural environment [17]. While it is possible to selectively immobilize an enzyme to one polymer block of a copolymer surface, how this process affects the wettability of the overall surface remains to be seen [10, 15]. Understanding the balance of hydrophilic and hydrophobic groups on copolymer surfaces is important and can be exploited for applications such as atmospheric water harvesting [18-19]. In

other uses, including those involving fabrics, it would be desirable to impart small amounts of hydrophilicity while retaining as much bulk water repellency as possible [20].

Here, a series of amphiphilic surfaces has been created containing different micelle densities in order to simultaneously maximize the orthogonal functions of water repellency and enzyme activity. The block copolymer used, polystyrene-block-poly(acrylic acid) (PS-b-PAA), has been shown to form a variety of aggregates in solution that can be cast onto surfaces as thin films [21-25]. PS-b-PAA was dissolved in toluene to form reverse micelles with a PAA core and PS corona and then spin coated. Prior studies of amphiphilic block copolymer films have outlined a strategy for tuning the amphiphilic surface ratio by mixing in varying amounts of a pure polymer to dilute the copolymer micelles formed in solution [26]. The ratio of hydrophobic to hydrophilic sites on the surfaces here was varied by adding pure hydrophobic PS to the block copolymer solution. While these strategies exist, there has yet to be a study on how the block copolymer surface composition affects orthogonal functions. By compiling contact angle and enzyme assay measurements at each composition, the range of surface compositions that simultaneously maximized both desired functions was determined.

2. Materials and Methods

2.1 Materials

Gold coated glass surfaces with dimensions 10 mm x 10 mm x 1 mm were purchased from EMF Corp. The chips had 100 nm of Au evaporated onto 5 nm of Ti. The PS-b-PAA block copolymer, M_n 16,000-3,500 and polydispersity index (PDI) 1.15, was purchased from Polymer Source. Polystyrene (average M_W 35,000), poly(sodium-4-styrenesulfonate) (PSS) average M_W ~70,000, absolute ethanol, toluene American Chemical Society (ACS) reagent grade ≥99.5%, dimethyl sulfoxide (DMSO), N-(3-Dimethylaminopropyl)-N'-ethylcarbodiimide hydrochloride crystalline (EDC) and sodium hydroxide pellets ACS reagent, ≥97.0% were purchased from Sigma Aldrich. Poly(ethyleneimine) (PEI) solution, 50% (w/v) in water was purchased from Fluka. Phosphate buffered saline (PBS) 0.1 M (10X) pH 7.4, 30% hydrogen peroxide and Tween 20 were purchased from Fisher Scientific. N-Hydroxysuccinimide (NHS) was purchased from ThermoFisher Scientific. Horseradish peroxidase (HRP), purified enzyme immunoassay (EIA) grade, was purchased from Worthington Biochemical Corporation. Resorufin, sodium salt – reference standard for the calibration curve was purchased from Life Technologies. Amplex Red reagent from Molecular Probes was dissolved in DMSO. After dilution to 0.01 M (1X) pH 7.4 with deionized (DI) water, the PBS was vacuum filtered with Millipore 0.22 μm filter paper to remove small particles. All other chemicals and reagents were used as received without further purification.

2.2 Instrumentation

UV/ozone cleaning of Au surfaces was performed with a Novascan PSD Series UV-ozone cleaning system. Agitation was performed using a Boekel Scientific model 130300 Jitterbug microplate shaker. Atomic force microscopy (AFM) images were collected on a Bruker Dimension Icon AFM operated in tapping mode with ScanAsyst at ambient temperature and pressure. Images were acquired with ScanAsyst-Air tips from Bruker with 70 Hz cantilever frequency, 0.4 N/m spring constant and 2 nm tip radius. The surface roughness, R_a, was calculated as the arithmetic average of the absolute values of the surface height deviations measured from the mean plane: $R_a = \frac{1}{N}\sum_{j=1}^{N}|Z_j|$ where Z is the surface height deviation from the mean plane and N is the number of points. AFM images and measurements were processed using Nanoscope Analysis version 1.50. Hydrostatic contact angles were measured using a Kruss DSA 100B sessile drop-shape analyzer. Contact angles were measured in triplicate, using 3 μL drops and fit using the Laplace-Young equation[27]. Formation of fluorescent product was monitored using a SpectraMax M5 multimodal plate reader from Molecular Devices, in top-read mode, at 25 °C and excitation/emission wavelengths of 530/590 nm.

2.3 Methods

2.3.1 Creating Mixed PS-b-PAA & PS Solutions

The PS-b-PAA block copolymer was dissolved in toluene and subsequently heated to 55 °C for 45 min to form spherical micelles. To the PS-b-PAA solution, different amounts of pure PS were added to create solutions with PS:PS-b-PAA mole ratios of 2:1, 5:1, 10:1 and 25:1. The mixed solution was then diluted with toluene for spin coating to have a final PS-b-PAA concentration of 0.83 mg/mL. Additionally, a 100% PS-b-PAA and a 10 mg/mL PS solution

(100% PS) were also prepared for spin-coating. These two solutions are referred to as "PS-b-PAA" and "PS" below. The PS surface underwent the same reaction, enzyme exposure and washing conditions as the surfaces with the copolymer. A schematic of the preparation can be seen in Figure 1.

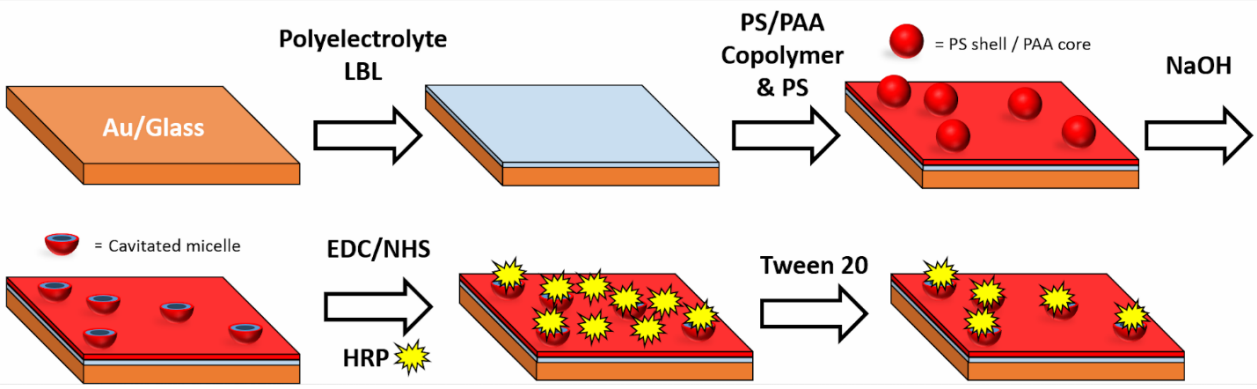

Figure 1. Schematic for the preparation of PS:PS-b-PAA polymer thin films with immobilized HRP.

2.3.2 Surface Cleaning Procedure

Surfaces were cleaned by sonicating in ethanol for 15 min, then rinsed with DI water, and dried with N_2. Further cleaning was accomplished by placing the surfaces in the UV/ozone cleaner for 15 min. Surfaces were rinsed with DI water and then immediately placed in the first DI water washing bath for the layer-by-layer process.

2.3.3 Layer-by-Layer and Spin-Coating Procedure

Before coating the Au chip with the copolymer film, a polyelectrolyte adhesion layer was formed to prevent the copolymer film from delaminating when soaking in the sodium hydroxide solution (NaOH/DI water) [22]. Poly(sodium-4-styrenesulfonate) served as the negatively charged polymer and poly(ethyleneimine) was the positively charged polymer. Solutions of both the anionic and cationic polymers were made separately at 1% (w/v) in DI water and DI water baths were used for washing. Au chips were soaked in each bath for 1 min followed by a 1 min soak in DI water bath for washing. Four bilayers of PSS/PEI were formed as the adhesion layer.

After cycling through the polyelectrolyte baths, the surfaces were rinsed with DI water and dried with N_2 prior to spin-coating. Polymer solutions in toluene were dispensed onto the surface once it was spinning at 1000 rpm and then ramped to 1600 rpm for 1 min. To measure film thickness, portions of the PS-b-PAA film were scratched off with tweezers and the AFM tip was scanned over the interface. To expose the acid groups of the PAA core to the air interface, surfaces were soaked in a NaOH/DI water solution at pH 9.5 for 10 min [22]. After rinsing with DI water and drying with N_2, the exposed acid groups were then converted to NHS ester groups.

2.3.4 Enzyme Immobilization and Assay

The free acid groups on the surface were converted to N-hydroxysuccinimide (NHS) ester groups via activation with EDC. Each surface was soaked for 10 min in 400 µL of a mixed solution of 0.1 M NHS and 0.4 M EDC dissolved in DI water. After 10 min, surfaces were rinsed with DI water and dried with N_2. HRP was immobilized to the surface via the reaction between the free primary amine group(s) of the HRP and the surface-bound NHS groups, forming a stable amide bond [28-29]. Polymer surfaces were immersed in 8.2 µg/mL HRP in PBS 0.01 M pH 7.4 for 60 min at 4 °C. To address non-specifically attached enzyme, surfaces were treated by rinsing with PBS 0.01 M pH 7.4 and DI water and then agitated in 0.1% (v/v) Tween 20 solution in PBS 0.01 M pH 7.4 for 30 min, replacing the Tween 20 solution every 10 min. After agitation, all surfaces were rinsed with PBS 0.01 M pH 7.4, DI water and then dried with N_2.

For the enzyme activity assay, the surfaces were placed in 350 µL of PBS 0.01 M pH 7.4. Enzyme activity was measured at 25 °C via the fluorescence of a reactively formed molecule, resorufin, from the decomposition of Amplex Red. In the presence of hydrogen peroxide, HRP catalyzes the reaction of Amplex Red (non-fluorescent) to resorufin (fluorescent), which has excitation/emission peaks at 530/590 nm, respectively [30]. The assay substrate was a 100 mM solution of Amplex Red in DMSO. After dissolving, a 1.11% (v/v) solution was made of the 100 mM Amplex Red in PBS 0.01 M pH 7.4. Separately, 30% hydrogen peroxide was dissolved in PBS 0.01 M pH 7.4 to make a 0.23% (v/v) solution. These solutions were prepared within 15 min of beginning the assay and kept covered as Amplex Red is light sensitive [31].

To commence the assay, the Amplex Red and peroxide solutions were mixed together, and 350 µL aliquots were added to each surface-containing microplate well. The well plate was mixed in the plate shaker for the duration of the assay. At specific time points, a 100 µL aliquot of the reaction solution was transferred to a 384 well microtiter plate to measure the fluorescence. Once fluorescence was measured, the aliquot was returned to the original sample well to keep the reaction solution volume constant. A resorufin/fluorescence calibration curve was generated by measuring the fluorescence of several different molarities of a reference standard resorufin sodium salt [32].

3. Results and Discussion

3.1 Determining Micelle Density

In order to maintain a balance of both functions on the surface, it was necessary to have a uniform mixing of the enzyme attachment sites (copolymer micelles) and the water repellent background (pure PS). To characterize the spatial distribution of the copolymer films on the nanoscale, AFM was used. With AFM, the shape of the micelles was verified, as well as the concentration on the surface for a particular solution composition. Figure 2A is an AFM topography image of the 100% block copolymer film spun on the polyelectrolyte adhesion layer from a toluene solution containing the dissolved PS-b-PAA after heating. From the image it is clear that spherical micelles did form and were cast onto the surface in a pseudo-hexagonal arrangement (inset). The color contrast of micelles in Figure 2 corresponds to height differences within the layer. According to previously reported studies, the size of the spherical micelle is dependent on the length of the insoluble block, overall molecular weight, solvent and temperature [1-2]. From a total of 7 μm^2 analyzed across two different chips prepared identically, the PS-b-PAA micelles measured 20.2 ± 9.4 nm in diameter. The mean size of these micelles is comparable to the diameter of micelles measured previously from a similarly sized block copolymer [21]. Size distributions can be attributed to the polydispersity of the copolymer and roughness in the underlying substrate. Having copolymer multilayers form after spin coating will also affect the measured size of the copolymer micelles as scanning effects will cause top layer micelles to image larger and wider than they really are [33]. The height of the block copolymer film, measured above the polyelectrolyte layer, was 62.2 ± 4.1 nm, which is roughly three times the diameter of a single micelle.

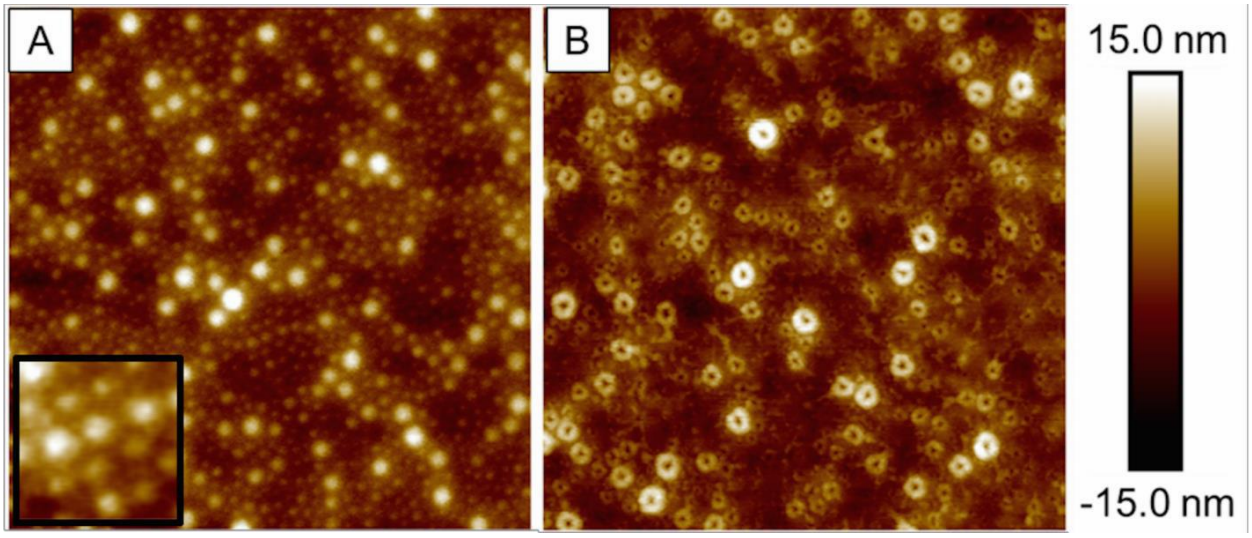

Figure 2. AFM topography images of a PS-b-PAA block copolymer film after spin coating (A) reveal spherical micelles. After soaking in NaOH solution (B) the spherical micelles have a depression in the middle, forming cavities. Images are 1 x 1 μm^2. Inset in (A) is zoomed in region showing the pseudo-hexagonal packing of the as-cast micelles. Inset is 0.1 x 0.1 μm^2.

To access the free acid groups on the PAA block and expose them to the air interface, it was necessary to "burst" the micelles. Micelle cavitation was accomplished by soaking the surfaces in a solution of NaOH in DI water at pH 9.5. The morphology and diameter of the micelles after soaking in a NaOH solution was noticeably different, as can be seen in Figure 2B. As-cast, the micelles imaged as homogeneous spheres but after soaking they displayed a cavity in the middle indicated by the depression in AFM images. After soaking in NaOH, the average diameter of the micelles swelled from 20.2 ± 9.4 nm to 29.1 ± 13.3 nm. The diameter of the cavitated micelles was calculated from 10 μm^2 analyzed over multiple surface compositions. Once cavitated, these micelles expose acid groups and function as "nano-reactors" for enzyme immobilization [21].

By multiplying the average micelle diameter by the micelle density, the coverage of micelles for a given surface composition can be calculated. In Figure 2B, the 100% PS-b-PAA surface is 17% covered by cavitated micelles. At this composition, the enzyme activity function may be favored at the detriment of the water repellency function because the exposed hydrophilic groups cover a large fraction of the surface. As a consequence, having a way to tune the density of attachment sites within the hydrophobic background was critical in finding the optimal composition that supported both functions simultaneously. It has been demonstrated that by mixing in a pure polymer, such as PS, it was possible to decrease the density of micelles on a surface [26].

With this approach, density of hydrophilic micelles on the hydrophobic surface was altered, and both functions were measured and the best surface composition for simultaneous optimization was determined. Pure PS was added to solutions of the micellized PS-b-PAA copolymer to yield solutions with PS:PS-b-PAA mole ratios of 2:1, 5:1, 10:1 and 25:1. Each of these solutions were used to spin coat multiple chips, which were then imaged with AFM after bursting in the NaOH pH 9.5 solution. Representative images from each surface composition are shown in Figure 3A-D. With these images it was evident that with increasing moles of pure PS added to the solution, from 2:1 in Figure 3A to 25:1 in Figure 3D, the density of PS-b-PAA micelles (bright spots) decreased. To calculate the surface micelle density, AFM images were collected from at least six areas on two separate chips per solution composition, totaling an area of at least 6 μm^2. Only micelles that had a circular shape with a size approximating the diameter measured above (29.1 ± 13.3 nm) were counted. The average micelle density and standard deviation are plotted in Figure 4 for all surface compositions containing PS-b-PAA micelles. Initially, there was a decrease in the micelle density from the 100% PS-b-PAA surface to the 2:1 surface from 262 ± 54 micelles/μm^2 to 51 ± 7 micelles/μm^2 respectively. With increasing moles of pure PS the micelle density ultimately decreased to 4 ± 1 micelles/μm^2 at the 25:1 surface. Having established a way of tuning the micelle concentration on the surface, it was next determined how the different micelle densities affected the overall enzymatic activity and water repellency of the surface.

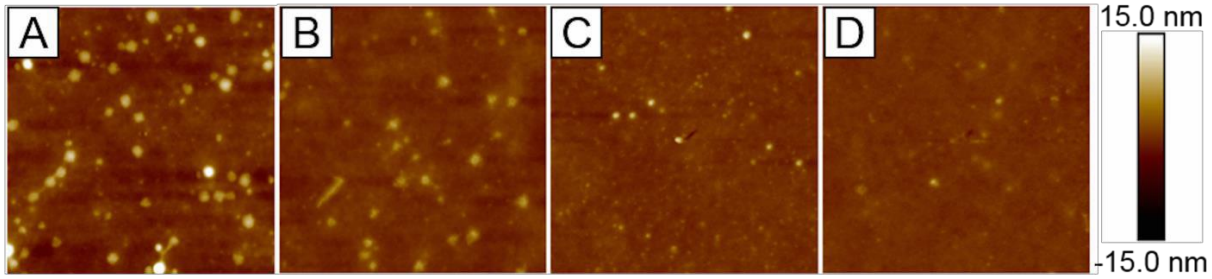

Figure 3. AFM topography images of surfaces cast from solutions containing different mole ratios of pure PS to the PS-b-PAA block copolymer. (A) 2:1 (B) 5:1 (C) 10:1 and (D) 25:1. All images are 1 x 1 μm^2.

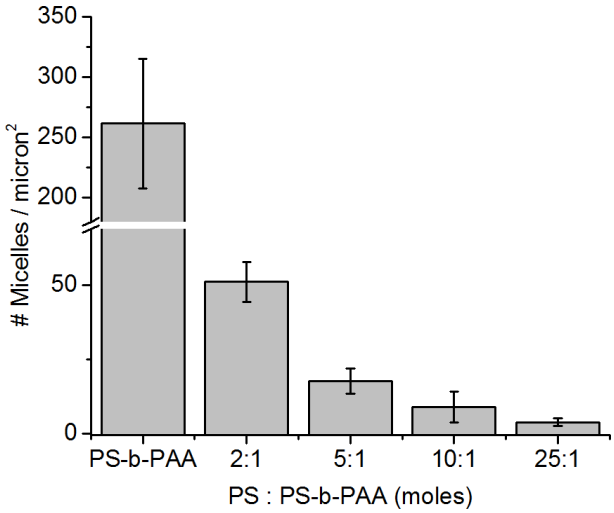

Figure 4. Micelle density as a function of PS:PS-b-PAA. The micelle density was determined by counting the number of micelles per area over 6 μm^2 for each solution on multiple chips. Error bars are the standard deviation of density measurements.

3.2 Measuring the Water Repellency Function

To measure the water repellency function, static sessile drop measurements of water were taken on the surfaces. In Figure 5 the contact angles are plotted as a function of the molar ratio of PS to the PS-b-PAA copolymer; filled squares, left y-axis. As expected, the surface with the highest density of micelles (PS-b-PAA) had the lowest contact angle at 58.9 ± 5.4°. However, by increasing PS content, thereby decreasing the micelle density, the contact angle increased until the 5:1 surface, when it converged at the same contact angle as the PS surface, 90°. By increasing the PS content it was clear that the overall hydrophobicity of the surface increased. However, this increase in contact angle could have resulted from higher surface roughness as well. From the AFM topography images, the average surface roughness, R_a, was calculated at each composition. The average surface roughness is plotted in Figure 5: open triangles, right y-axis. While it is possible to increase the contact angle via increasing the physical surface roughness [12], it was found that the surface actually became smoother with increasing PS content, and therefore the increasing contact angle resulted from the chemical nature of PS.

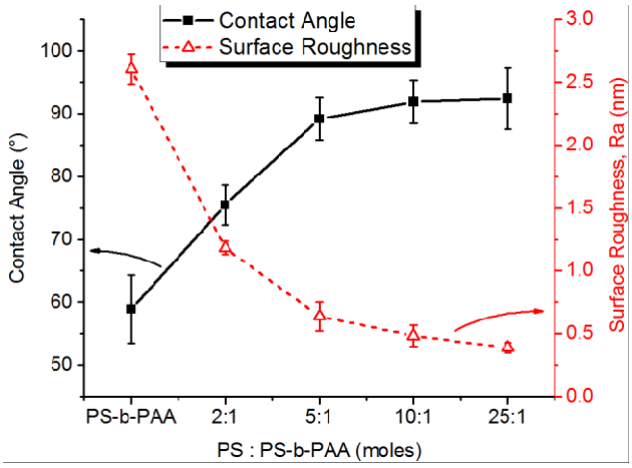

Figure 5. Left Y axis, contact angle measurements for different PS:PS-b-PAA ratios after spin coating and soaking in NaOH. Right Y axis, roughness measurements collected via AFM. The arrows in the graph point to the appropriate axis for each set of data points. Error bars are the standard deviation of the measurements for each data point.

One major concern with immobilizing enzymes to these surfaces was the non-specific adsorption, or bio-fouling, of enzyme to the hydrophobic areas between the micelles. Typically, surfaces that resist bio-fouling have zwitterionic or ethylene glycol groups, but these are hydrophilic rather than hydrophobic [34]. In prior work, it was shown that it was possible to remove significant non-specifically bound enzyme from an amphiphilic surface containing fluorinated groups by washing with a surfactant, Tween 20 [32]. After soaking in a HRP/PBS solution, the copolymer surfaces were washed in a 0.1% (v/v) Tween 20/PBS solution 0.01 M pH 7.4 to attempt to remove non-specifically bound enzyme.

After washing, the contact angles were re-measured to verify that the surface remained water repellent after enzyme immobilization. The contact angles for each surface composition ranging from 100% to 0% PS-b-PAA are plotted in Figure 6. From this plot, there was a significant decrease in the contact angle of all the surfaces after exposure to HRP and washing. As with the Pre-HRP data points, the same general trend existed in the Post-HRP contact angles; the contact angle increased from PS-b-PAA to PS and plateaued between the 2:1 and 5:1 surfaces. A decrease in the contact angle was expected since enzyme was covalently immobilized to the surface, (PS-b-PAA surface, Figure 6). However, the decrease in the contact angle of the 100% PS surface in Figure 6 indicated there was fouling from the enzyme that was not removed by washing. Even though it decreased, the 100% PS surface did retain 85% of the Pre-HRP contact angle, decreasing from 90.3 ± 2.0° to 77.2 ± 5.3°. The 5:1, 10:1 and 25:1 surfaces decreased to an even greater extent than the 100% PS surface, likely due to the additive effect of enzyme immobilization and non-specific enzyme binding. Even though a decrease in contact angle was observed for all the surfaces, there was still a discernable plateau reached between the 2:1 and 5:1 surfaces. From those contact angle measurements, it can be concluded that the first function of water repellency was maximized on surfaces with a PS:PS-b-PAA ratio greater than 2:1.

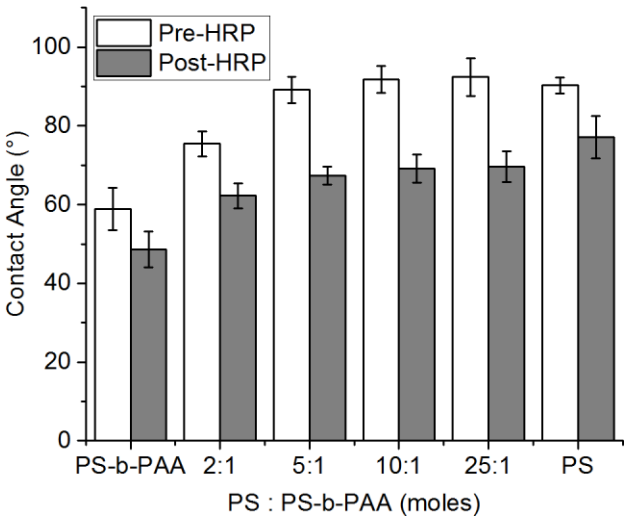

Figure 6. Contact angle measurements pre- (white) and post- (gray) exposure to HRP and washing. In the Post-HRP data set, the contact angle is plateauing between the 2:1 and 5:1 surfaces. Error bars are the standard deviation of the measurements for each data point.

3.3 Measuring the Enzyme Activity Function

For the second function, enzyme activity, the activity of the immobilized HRP via fluorescence assay was measured. In Figure 7, the measured fluorescence, in relative fluorescence units (RFU), is plotted for each solution at the specified time points. Surprisingly, it was observed that the 100% PS-b-PAA surface did not produce the highest activity even though it had the highest micelle surface concentration (Figure 4). The diminished activity on the 100% PS-b-PAA surface can be attributed to deactivation of immobilized enzyme molecules caused by steric hindrance and crowding. In a similar system where enzymes were immobilized to PAA groups in a copolymer membrane, hindrance and crowding were suggested to explain the observed decrease in immobilized enzyme activity at high loading [10]. As site-selective enzyme immobilization of the HRP was not used, it is possible for there to be multiple points on the enzyme that bound to the surface, causing deactivation. As the number of immobilization sites on the surface decreased, the probability of one enzyme binding via more than one site would also have decreased. Once the strain and crowding had been relieved by decreasing the micelle density on the 2:1 surface (Figure 2B to 3A), the enzyme activity significantly increased (Figure 7).

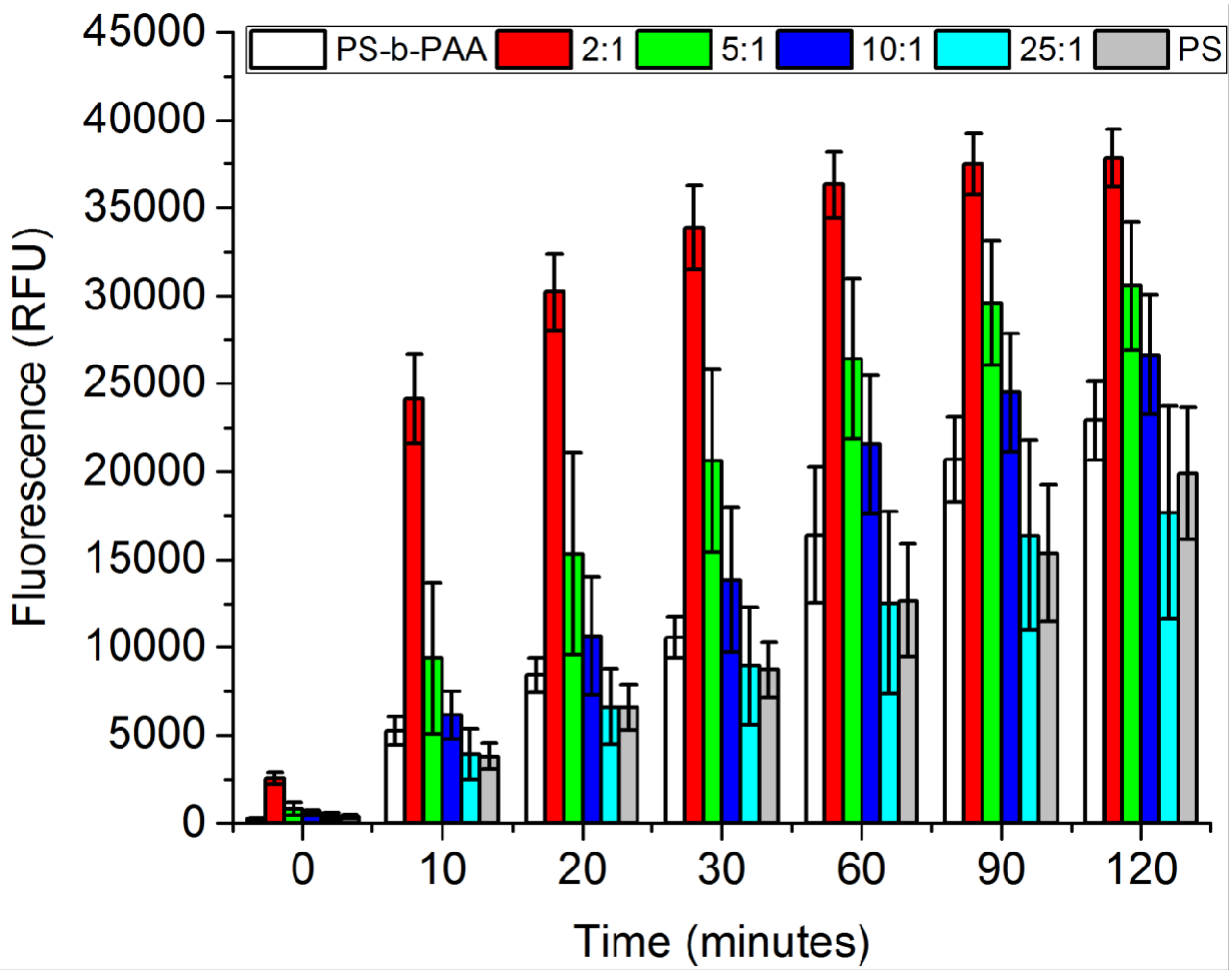

Figure 7. HRP fluorescence assay for the different PS:PS-b-PAA surfaces. Fluorescence, measured in RFU, was collected at specified time points for all surfaces. Error bars are the standard deviation of the mean.

Beyond the 2:1 surface, the measured enzyme activity decreased, following the same trend as the micelle concentration (Figure 4). The measured activity decreased after 2:1 until 25:1, which was not statistically different than the 100% PS control surface. Since the contact angle measurements in Figure 6 suggested that there was HRP non-specifically bound to the 100% PS surface, it was included in the assay to determine if it had measurable fluorescence. Compared to the fluorinated control surface in the previous work, the 100% PS surface had higher measured enzyme activity, indicating poorer resistance to fouling and washing [32]. Based on the assay results in Figure 7, it was determined that the only surfaces with a fluorescence signal greater than the negative control surface (100% PS) were the 2:1, 5:1 and 10:1 surfaces. Therefore, the 2:1, 5:1 and 10:1 surfaces successfully achieved the second function of measureable enzyme activity.

3.4 Determining Surface Composition Needed for Simultaneous Multifunctionality

To determine the surface compositions that provided the optimal simultaneous multifunctionality, the fluorescence intensity from Figure 7 was first converted into moles of the reactively formed product, resorufin. A 60 min reaction time was selected for this conversion because at that time point the most active surface, 2:1, had plateaued. The conversion of RFU to moles was accomplished using a calibration curve of resorufin solutions at different concentrations [32]. The moles of reactively formed resorufin are plotted as a function of surface composition in Figure 8, left y-axis. For comparison, the contact angles for the same surface compositions after soaking in HRP and washing are plotted on the right y-axis of Figure 8. From the contact angle measurements taken before and after exposure to HRP, it was observed that while there was fouling, the contact angle peaked at 62.3 ± 3.2° by the 2:1 surface and leveled off up to the 25:1 surface. Since the 2:1 - 25:1 surfaces had roughly identical contact angles, the enzyme activity was the function used to determine the ultimate multifunctional compositions. From the amount of reactively formed resorufin for those four surfaces, only the 2:1, 5:1 and 10:1 surfaces had measurable enzyme activity above the minimum threshold described above. By these guidelines, the 2:1, 5:1 and 10:1 surfaces (and those contained within that range) successfully achieved water repellency and enzyme activity simultaneously.

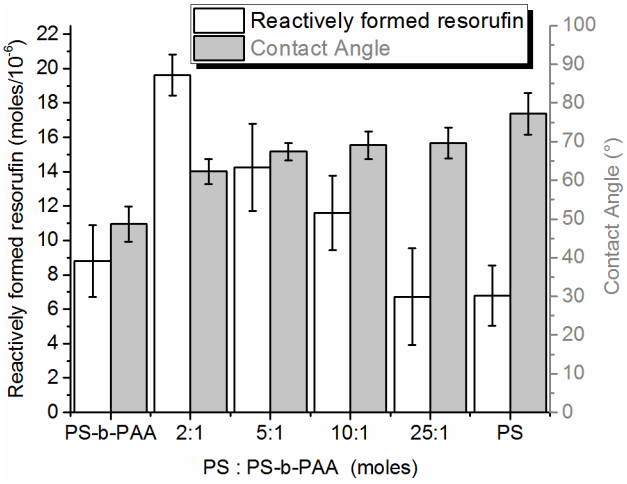

Figure 8. Comparison of the total product formed during 60 min reaction time, in moles (Left Y axis) and the contact angle after HRP immobilization and washing (Right Y axis). Error bars are the standard deviation of the measurements for each data point.

Even though the 2:1, 5:1 and 10:1 surfaces were identified as surface compositions that were multifunctional, there are still opportunities to improve them. These surfaces achieved the highest level of water repellency attainable after exposure to the enzyme, but had a contact angle below 90° and cannot be considered hydrophobic [27]. The decrease in the contact angle was attributed to non-specific binding of the HRP to the polystyrene leading to biofouling. While, to the knowledge of the project team, this is the first example of an amphiphilic block copolymer film that simultaneously balanced these orthogonal functions, it would be possible to improve upon it with a fluorinated polymer additive or a fluorinated copolymer system [35]. Replacing the polystyrene with a fluorinated polymer should reduce biofouling and increase overall

hydrophobicity, as shown in the team's previous work on multifunctional surfaces using a mixed thiol system [32].

4. Conclusion

In this work, it was established that the highest enzyme activity did not occur at the highest micelle density, but rather at an intermediate concentration. By decreasing the micelle concentration, the steric hindrance can be reduced, as can the likelihood of having multidentate enzyme binding to the surface, both of which can cause deactivation. For the water repellency function, the composition with the highest contact angle after enzyme immobilization was found. From contact angle and enzyme activity results, the team was able to demonstrate that the 2:1, 5:1 and 10:1 surfaces maximized both orthogonal functions simultaneously.

These results build on previous reports [10, 15, 26] of functionalized copolymer surfaces, which often look at only one function, by making a block copolymer thin film that simultaneously balances two orthogonal functions. The use of an amphiphilic block copolymer as the multifunctional thin film was also advantageous because it was possible to create small, uniformly dispersed nanoreactors that approached the size of a single enzyme molecule [36]. Additionally, block copolymers with immiscible blocks are able to form micelles with a range of morphologies via self-assembly that could be explored for multifunctionality [2]. By tuning the density of block copolymer micelles on a surface at the nano-scale to vary the ratio of hydrophobicity to hydrophilicity on an amphiphilic surface, the project team has, for the first time, simultaneously balanced the orthogonal functions of enzyme activity and water-repellency.

Unfortunately, some biofouling was observed on the PS portions of all the surfaces, leading to a decrease in the contact angle after enzyme exposure and washing. Going forward with a different hydrophobic polymer, the ratios of hydrophobic and hydrophilic sites between the 2:1 and 10:1 surfaces are promising towards achieving an improved simultaneous multifunctional surface that balances the orthogonal functions of enzyme activity and water repellency. A surface capable of balancing these functions would see application in creating multifunctional fabrics and textiles [20, 37].

This document reports research undertaken at the U.S. Army Natick Soldier Research, Development and Engineering Center, Natick, MA, and has been assigned No. NATICK/TR- 18/014 in a series of reports approved for publication.

5. References

[1] R. Nagarajan, K. Ganesh, *Journal of Chemical Physics* **1989**, *90*, 5843-5856.
[2] Y. Mai, A. Eisenberg, *Chemical Society Reviews* **2012**, *41*, 5969-5985.
[3] G. Riess, *Progress in Polymer Science* **2003**, *28*, 1107-1170.
[4] Q. Chen, H. Schoenherr, G. J. Vancso, *Small* **2009**, *5*, 1436-1445.
[5] Q. Chen, G. W. de Groot, H. Schonherr, G. J. Vancso, *European Polymer Journal* **2011**, *47*, 130-138.
[6] M. Q. Li, C. K. Ober, *Materials Today* **2006**, *9*, 30-39.
[7] T. Pietsch, P. Mueller-Buschbaum, B. Mahltig, A. Fahmi, *ACS Applied Materials & Interfaces* **2015**, *7*, 12440-12449.
[8] R. D. Bennett, G. Y. Xiong, Z. F. Ren, R. E. Cohen, *Chemistry of Materials* **2004**, *16*, 5589-5595.
[9] J.-i. Hahm, *Langmuir* **2014**, *30*, 9891-9904.
[10] L. Ying, E. T. Kang, K. G. Neoh, *Journal of Membrane Science* **2002**, *208*, 361-374.
[11] J. Malmstroem, J. Travas-Sejdic, *Journal of Applied Polymer Science* **2014**, *131*.
[12] Y. Zhu, M. Shi, X. Wu, S. Yang, *Journal of Colloid and Interface Science* **2007**, *315*, 580-587.
[13] S. G. Im, K. W. Bong, B.-S. Kim, S. H. Baxamusa, P. T. Hammond, P. S. Doyle, K. K. Gleason, *Journal of the American Chemical Society* **2008**, *130*, 14424-14425.
[14] S. A. Bhakta, T. E. Benavidez, C. D. Garcia, *Journal of Colloid and Interface Science* **2014**, *430*, 351-356.
[15] O. Parajuli, A. Gupta, N. Kumar, J.-i. Hahm, *Journal of Physical Chemistry B* **2007**, *111*, 14022-14027.
[16] C. Mateo, J. M. Palomo, G. Fernandez-Lorente, J. M. Guisan, R. Fernandez-Lafuente, *Enzyme and Microbial Technology* **2007**, *40*, 1451-1463.
[17] P. V. Iyer, L. Ananthanarayan, *Process Biochemistry* **2008**, *43*, 1019-1032.
[18] S. C. Thickett, C. Neto, A. T. Harris, *Advanced Materials* **2011**, *23*, 3718-3722.
[19] E. Ueda, P. A. Levkin, *Adv. Mater.* **2013**, *25*, 1234-1247.
[20] K. Sasaki, M. Tenjimbayashi, K. Manabe, S. Shiratori, *ACS Applied Materials & Interfaces* **2016**, *8*, 651-659.
[21] Y. Boontongkong, R. E. Cohen, *Macromolecules* **2002**, *35*, 3647-3652.
[22] A. C. Miller, R. D. Bennett, P. T. Hammond, D. J. Irvine, R. E. Cohen, *Macromolecules* **2008**, *41*, 1739-1744.
[23] L. F. Zhang, A. Eisenberg, *Science* **1995**, *268*, 1728-1731.
[24] C. Xu, B. B. Wayland, M. Fryd, K. I. Winey, R. J. Composto, *Macromolecules* **2006**, *39*, 6063-6070.
[25] D. E. Discher, A. Eisenberg, *Science* **2002**, *297*, 967-973.
[26] R. D. Bennett, A. C. Miller, N. T. Kohen, P. T. Hammond, D. J. Irvine, R. E. Cohen, *Macromolecules* **2005**, *38*, 10728-10735.
[27] K. W. Kolasinski, John Wiley & Sons, Ltd, **2012**.
[28] J. Lahiri, L. Isaacs, J. Tien, G. M. Whitesides, *Anal. Chem.* **1999**, *71*, 777-790.
[29] N. Patel, M. C. Davies, M. Hartshorne, R. J. Heaton, C. J. Roberts, S. J. B. Tendler, P. M. Williams, *Langmuir* **1997**, *13*, 6485-6490.
[30] M. J. Zhou, Z. J. Diwu, N. Panchuk-Voloshina, R. P. Haugland, *Anal. Biochem.* **1997**, *253*, 162-168.

[31] B. Zhao, F. A. Summers, R. P. Mason, *Free Radical Biol. Med.* **2012**, *53*, 1080-1087.
[32] T. J. Lawton, J. R. Uzarski, S. F. Filocamo, *Chemistry – A European Journal* **2016**, *22*, 12068-12073.
[33] D. Ricci, P. C. Braga, in *Atomic Force Microscopy: Biomedical Methods and Applications* (Eds.: P. C. Braga, D. Ricci), Humana Press, Totowa, NJ, **2004**, pp. 25-37.
[34] E. Ostuni, R. G. Chapman, M. N. Liang, G. Meluleni, G. Pier, D. E. Ingber, G. M. Whitesides, *Langmuir* **2001**, *17*, 6336-6343.
[35] J. Gao, D. H. Yan, H. G. Ni, L. Wang, Y. H. Yang, X. P. Wang, *Journal of Colloid and Interface Science* **2013**, *393*, 361-368.
[36] J. D. Zhang, Q. J. Chi, S. J. Dong, E. K. Wang, *Bioelectrochemistry and Bioenergetics* **1996**, *39*, 267-274.
[37] P. Malshe, M. Mazloumpour, A. El-Shafei, P. Hauser, *Surface & Coatings Technology* **2013**, *217*, 112-118.